Wiener Chaos Random Fourier Series as a Tool to Study the Coupling of Noise with Power System Transient Response

Xingrui Li, *Student member, IEEE,* Chengxi Liu, *Senior Member, IEEE,* Chenxu Wang, Muhammad Adeen, *Member, IEEE,* Rodrigo Bernal, and Federico Milano, *Fellow, IEEE*

***Abstract*—This letter studies the impact of the frequency spectrum of stochastic processes on the transient behavior of dynamic power systems. The Wiener Chaos Random Fourier Series technique is utilized to first decompose the noise into a series of harmonics with same statistical properties as the original process and then analyze the influence of specific frequency regions of the spectrum of the stochastic processes on the system transient response and stability. Simulation results show that the coupling between noise and system dynamics does not necessarily occur in the range of frequencies of the critical modes. These results are illustrated and duly interpreted through the Kundur's two-area system.**

***Index Terms*—Stability analysis, stochastic differential equations (SDEs), Ornstein-Uhlenbeck's process (OUP), Wiener Chaos Random Fourier Series (WCRFS).**

I. Introduction

In recent years, a variety works have focused on the impact of the stochastic disturbances on the transient behavior of power systems [1]. In [2] and [3], the dynamic response of the grid is studied by adjusting the standard deviation or auto-correlation coefficient of the stochastic process. These references show that the auto-correlation amplifies the amplitude of the whole frequency spectrum of the stochastic processes, eventually worsening the oscillations of the critical modes of the system. However, which part of the harmonic content of the noise causes system instability is not discussed. In [4], forced oscillations caused by stochastic disturbances are injected into the system through a frequency window centered in the system critical mode. The approach in [4], known as power spectral density (PSD), does not fully capture the statistical properties of the stochastic processes and, hence, does not reproduce well the overall dynamic response of system nor its instabilities. Moreover, The PSD does not allow to properly capture the autocorrelation of the stochastic process if a certain frequency window is removed. In [5], the probability of system frequency deviation being in the security range is obtained by calculating the mean and variance of frequency changes. However, the technique proposed in [5] is not applicable when some simulations are terminated midway due to a serious event, such as voltage collapse. Also, in [4] and [5], the system models are linearized and, hence, cannot capture saturations, grazing and other nonlinear phenomena. In [6] and [7], the uncertainty propagation of the stochastic inputs is quantified efficiently. However, disturbances are assumed to be small and, as a result, the system is always stable. In [8], the Gaussian and non-Gaussian stochastic excitations are modeled, but the auto-correlation and the instabilities that arise with harmonic resonances are not studied.

This letter addresses the limitations of the approaches above and discusses the dynamic coupling between specific regions of the frequency spectrum of stochastic processes and system stability. With this aim, the proposed method utilizes the Wiener Chaos Random Fourier Series (WCRFS) to model stochastic processes. The proposed formulation fully retains the nonlinearity of the system and allows reproducing accurately the standard deviation, autocorrelation and harmonic content of the original processes. Then, specific frequency regions are removed from the WCRFS models and the impact of the lack of these regions is studied through time domain simulations.

X. Li and C. Liu are with Hubei Engineering and Technology Research Center for AC/DC Intelligent Distribution Network, School of Electrical Engineering and Automation, Wuhan University, Wuhan 430072, China.

C. Wang is with State Grid Zhejiang Electric Power Research Institute, Hangzhou 310014, China.

R. Bernal and F. Milano are with School of Electrical & Electronic Engineering, University College Dublin, Dublin, D04V1W8, Ireland.

M. Adeen is with EirGrid plc, D04FW28, Dublin, Ireland.

This work is partly supported by the China Scholarship Council (CSC) by funding X. Li for 1-year study at the University College Dublin; the National Natural Science Foundation of China (NSFC) by funding C. Liu under project 52007133; and the Sustainable Energy Authority of Ireland (SEAI) by funding F. Milano and R. Bernal under project FRESLIPS, Grant No. RDD/00681.

II. Modeling

Power systems subject to noise can be modeled as a set of stochastic differential-algebraic equations (SDAEs) [1], as follows:

$$\dot{\boldsymbol{x}} = \boldsymbol{f}(\boldsymbol{x}, \boldsymbol{y}, \boldsymbol{\kappa}) \,, \tag{1}$$

$$\boldsymbol{0} = \boldsymbol{g}(\boldsymbol{x}, \boldsymbol{y}, \boldsymbol{\kappa}) \,, \tag{2}$$

$$\dot{\boldsymbol{\kappa}} = \boldsymbol{a}(\boldsymbol{\kappa}) + \boldsymbol{b}(\boldsymbol{\kappa}) \circ \boldsymbol{\xi} \,. \tag{3}$$

Equations (1) and (2) model the conventional deterministic part of the dynamic power system. $\boldsymbol{f} : \mathbb{R}^{l+m+n} \mapsto \mathbb{R}^{l}$ are the differential equations; $\boldsymbol{g} : \mathbb{R}^{l+m+n} \mapsto \mathbb{R}^{m}$ are the algebraic equations; $\boldsymbol{x} \in \mathbb{R}^{l}$ is a vector of state variables; $\boldsymbol{y} \in \mathbb{R}^{m}$ is a vector of algebraic variables. In (3), $\boldsymbol{\kappa} \in \mathbb{R}^{n}$ represents the vector of stochastic processes; $\boldsymbol{\xi} \in \mathbb{R}^{n}$ is a vector of n-dimensional Gaussian white noise that represents the time derivative of the Wiener process; and $\circ$ represents the element-by-element product of vectors. Stochastic processes are defined by a drift, $\boldsymbol{a} : \mathbb{R}^{n} \mapsto \mathbb{R}^{n}$, and a diffusion term, $\boldsymbol{b} : \mathbb{R}^{n} \mapsto \mathbb{R}^{n}$. Proper characterization of $\boldsymbol{a}$ and $\boldsymbol{b}$ allows reproducing the probability distribution and autocorrelation of the stochastic processes [9].

1) Ornstein-Uhlenbeck's Process: The Ornstein-Uhlenbeck's process (OUP), also known as the stationary mean-reverting process, is used in this letter to model the stochastic disturbance. The OUP has been widely implemented in the literature to model the stochastic behaviors caused by physical processes, such as stochastic loads and short-term wind speed fluctuations [9], [10]. The SDE defining the OUP has the following form:

$$\dot{\kappa} = -\alpha \left(\kappa - \mu\right) + \beta \, \xi \,, \tag{4}$$

where α is the autocorrelation coefficient; β is the coefficient of the diffusion term; μ is the mean value; and ξ is the white noise. If κ is a real-valued process following a Gaussian probability distribution given by $\mathcal{N}(\mu, \sigma^2)$, where σ is the standard deviation, then $\beta = \sigma\sqrt{2\alpha}$.

2) Wiener Chaos Random Fourier Series: Wiener Chaos Expansion (WCE) consists of two parts: Wiener Chaos Random Fourier Series (WCRFS) and Polynomial Chaos Expansion (PCE) [11]. WCRFS transforms the SDE to differential equations with a set of random variables. PCE is utilized to obtain the probabilistic features of the system response efficiently. In this letter we use only the WCRFS as a tool to approximate the stochastic process

with a given number of harmonics. Different from the deterministic Fourier transformation and Hilbert Huang transformation, WCRFS is an extension of the traditional Fourier transformation in the field of stochastic processes theory. According to the WCRFS theorem, the Gaussian random variable ξ_i can be expressed as:

$$\xi_i = \int_0^t m_i(s)\, dW(s)\,, \tag{5}$$

where $W(s)$ is a Wiener process $\{W(s), 0 \leq s \leq t\}$; $m_i(s), i = 0, 1, 2, ...$, are a set of complete orthonormal basis in the Hilbert space $L^2([0,t])$, as follows:

$$m_i(s) = \begin{cases} \frac{1}{\sqrt{t}}\,, & i = 0\,, \\ \sqrt{\frac{2}{t}}\cos(\frac{i\pi s}{t})\,, & i \geq 1\,. \end{cases} \tag{6}$$

Note that the orthonormal basis is not unique. It can also be chosen based on the eigenvalues and eigenfunctions of stochastic process known as Karhunen-Loeve Expansion [12] or based on Haar wavelets known as Levy-Ciesielski construction of the Wiener process [13].

Then, $W(s)$ can be orthogonally decomposed as a linear combination of random variables ξ_i that follow independent and identically distributed standard Gaussian distribution:

$$W(s) = \int_0^t \chi_{[0,s]}(\tau)\, dW(\tau) = \sum_{i=0}^{\infty} \xi_i \int_0^s m_i(\tau)\, d\tau\,, \tag{7}$$

where $\chi_{[0,s]}(\tau) = \sum_{i=0}^{\infty} m_i(\tau) \int_0^s m_i(\tau)\, d\tau$ is the characteristic function of interval $[0, s]$. For a given truncated order K, the derivative form of (7) can be approximated with:

$$dW(s) \approx \sum_{i=0}^{K} \xi_i m_i(s)\, ds\,. \tag{8}$$

The SDE model (3) can be transformed into an ordinary differential equation with random variables ξ_i using (8). Since ξ_i is fixed at the beginning of simulations, the Wiener process is projected onto $L^2[0,t]$ for a fixed time $t > 0$. Moreover, the relationship between the stochastic process and the corresponding frequency spectrum is built by the deterministic coefficients (6). This allows easily isolating the frequency band that triggers system instability by setting to zero the coefficients of the harmonics in a given range of the expansion. The first term of (8), i.e., the term $i = 0$, represents the *direct component* of the Wiener processes. The terms for $i \geq 1$ are called *alternating components*. In this letter, the truncation order K is chosen based on the following requirements: (i) the approximated moments using WCRFS are close to the moments of the original OUP; and (ii) the alternating components of WCRFS contain all system resonant frequencies. Condition (i) guarantees that WCRFS has statistical properties similar to the original stochastic process. Condition (ii) allows capturing the instabilities due to forced oscillations induced by stochastic processes.

III. Case Study

The well-known Kundur's two-area system is considered in this section. Two cases where stochastic loads are connected to Areas 1 and 2 respectively are studied. The first case serves to illustrate the features of the proposed method by comparing the accuracy with the Monte Carlo method (MC) which is set as benchmark. The second case demonstrates the performance of WCRFS when instability occurs in the system. Moreover, for Case 2, we show how to use the frequency decomposition of the WCRFS model to identify the parts of the noise spectrum that couple dynamically with the critical modes of the system.

Wiener processes are integrated with the Euler-Maruyama method with step size $h = 0.01$ s, while the drift term and deterministic DAEs are integrated using the trapezoidal method with $\Delta t = 0.01$ s. The total simulation time is set to 200 s. 1000 time-domain simulations are carried out in both WCRFS and MC methods. All simulations are carried out using the power system analysis software tool Dome [14]. The types of synchronous machines and AVRs are the same as those described in [15].

A. Case 1: Stochastic Load in Area 1

A stochastic load is connected to bus 7 of the two-area system. The means of active and reactive power consumption of the stochastic load are set equal to the initial value and standard deviations are $\sigma = 0.4\%$ of the means. To verify the correctness and compare the approximation accuracy of WCRFS, two scenarios, namely $\alpha = 0.1$ Hz and 1 Hz, are discussed. For each scenario, the order of WCRFS is set to 5, 50 and 500 respectively. In all scenarios, the mean values and autocorrelations of all WCRFS models are highly accurate and are thus not discussed below.

By setting the results of MC as the benchmark, the Average Absolute Error (AAE) e is used as performance comparison index:

$$e = \frac{\sum_{i=1}^{N} \left| u_i^{\mathrm{MC}} - u_i^{\mathrm{WCRFS}} \right|}{N} \tag{9}$$

where u_i^{MC} and u_i^{WCRFS} are statistical moments (e.g., mean or standard deviation) of the variables obtained with MC and WCRFS at the i-th time step, respectively; and N is the total number of steps.

For the discussion presented in this section we consider the active and reactive load consumptions at bus 7 (P_{L7}, Q_{L7}), that is, the quantities the Wiener stochastic processes of which are directly expanded through the WCRFS. The AAE comparison of the stochastic load for different autocorrelations and orders of WCRFS is summarized in Table I. In this table, mean and standard deviation are indicated with M. and S.D, respectively. The mean of both P_{L7} and Q_{L7} is accurate, as expected. The WCRFS, in fact, only modifies the diffusion term of the Wiener process while retaining the drift term, which includes the information on the mean value. Since the mean is not altered by WCRFS, the AAE of the mean can be regarded as an error caused by the uncertainty of the stochastic process itself. For an expansion order equal to 500, the AAE of the standard deviation is of the same magnitude as that of the mean, thus it can be considered that the process using WCRFS captures all the relevant features of the original process at this time. Also, the AAE of standard deviation decreases as the order of the WCRFS increases. This is a consequence of the convergence of the WCRFS. Note also that, as α increases, the accuracy of the standard deviation decreases. This happens because a bigger α leads to bigger amplitudes of the frequency spectrum [2], and, consequently, high-frequency components, which are truncated in low-order WCRFSs, have a non-negligible impact on the stochastic process.

Since the results for state variables and algebraic variables are similar, only the rotor speed of synchronous generator G2 (ω_2) and the voltage amplitude of bus 3 (v_3) are selected as representatives of state variables and algebraic variables respectively. The evolution of the standard deviation using WCRFS and MC when $\alpha = 0.1$ Hz and 1 Hz are shown in Figs. 1 and 2, respectively. The error between WCRFS and MC decreases as the order of the WCRFS increases, as expected. Moreover, the higher the WCRFS order, the more small fluctuations of ω_2 and v_3 are correctly captured during the simulation. In addition, an increase in α leads to a decrease in the accuracy as that of stochastic inputs. Finally, different variables have different sensitivities to the WCRFS order. For example, the accuracy of ω_2 using 50-th order WCRFS is relatively high in the upper panel of Fig. 2, while that of v_3 is lower in the lower panel of Fig. 2. Note

that each realization *per se* of MC and WCRFS might look different, see, e.g., Fig. 1 and Fig. 2. However, what really matters are the statistical properties, and these are substantially the same for the MC and the WCRFS with 500 harmonics.

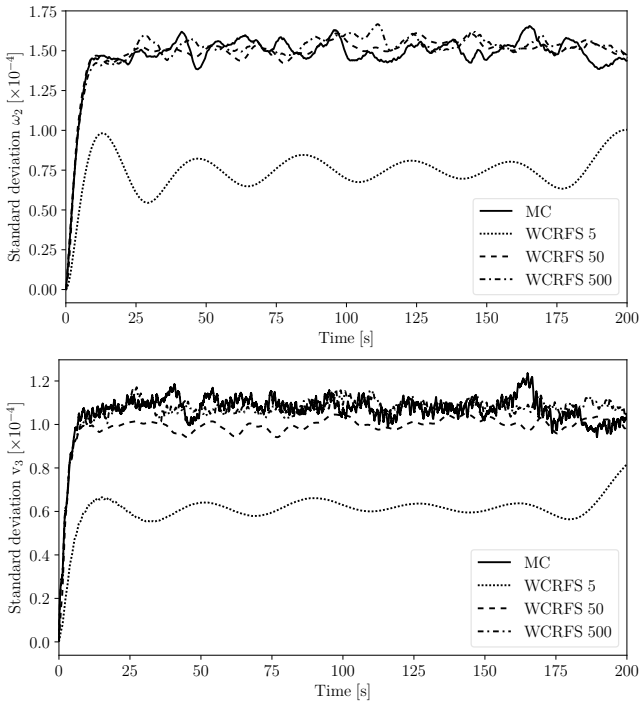

Fig. 1. Comparison of the standard deviation of the MC and WCRFS of orders from 5 to 500 for $\alpha = 0.1$ Hz. Upper panel: rotor speed of machine 2; Lower panel: voltage magnitude at bus 3.

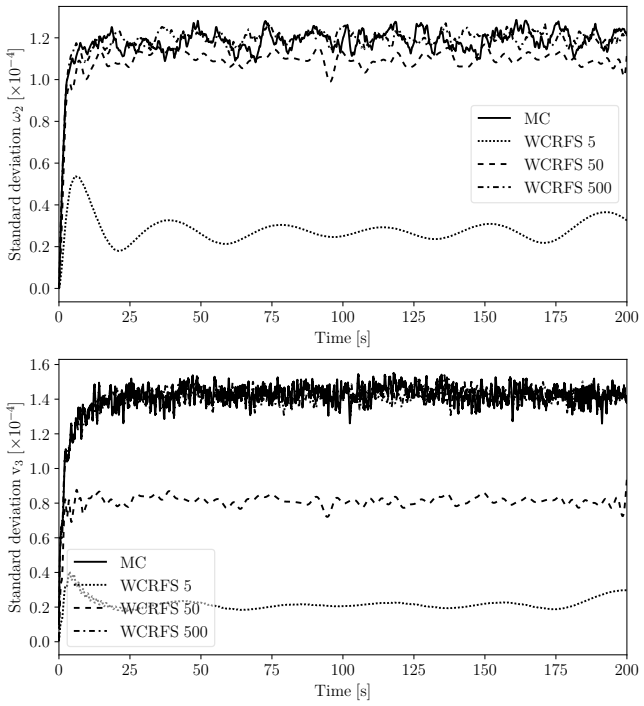

Fig. 2. Comparison of the standard deviation of the MC and WCRFS of orders from 5 to 500 for $\alpha = 1$ Hz. Upper panel: rotor speed of machine 2; Lower panel: voltage magnitude at bus 3.

TABLE I
AAE OF THE STOCHASTIC LOAD IN DIFFERENT AUTOCORRELATION AND ORDERS OF WCRFS

Method	α	K	$e_{P_{L7}}[\times 10^{-3}]$		$e_{Q_{L7}}[\times 10^{-4}]$	
			M.	S.D.	M.	S.D.
WCRFS	0.1	5	1.63	11.89	2.18	12.69
WCRFS	0.1	50	2.06	1.57	1.78	1.93
WCRFS	0.1	500	1.88	1.27	2.12	1.28
WCRFS	1	5	1.47	28.95	1.43	30.18
WCRFS	1	50	1.60	13.18	1.61	13.74
WCRFS	1	500	1.63	1.70	1.60	1.89

TABLE II
COMPARISON BETWEEN MC AND WCRFS MODELS OF DIFFERENT ORDERS

Method	Order	Freq. upper bound [Hz]	# of unstable trajectories
MC	–	–	290
WCRFS	140	0.350	3
WCRFS	150	0.375	9
WCRFS	160	0.400	56
WCRFS	170	0.425	188
WCRFS	180	0.450	243
WCRFS	190	0.475	263
WCRFS	200	0.500	264
WCRFS	210	0.525	268
WCRFS	500	1.250	286

B. Case 2: Stochastic Load in Area 2

In this case, the noise introduced by the load triggers unstable oscillations. We use this case to illustrate the ability of the proposed WCRFS model of the processes to identify which frequencies couple with the critical modes of the system. The mean, standard deviation, and autocorrelation of the stochastic load in bus 9 are set to the initial value, $\sigma = 0.6\%$ of the mean and $\alpha = 0.5$ Hz, respectively.

Table II shows the number of unstable trajectories using MC and WCRFS models of different orders. The corresponding frequency upper bound of a given order of WCRFS is calculated using (6). The dominant electro-mechanical modes of the system and corresponding frequency, damping and most participating area are shown in Table III. We consider WCRFS up to the 500-th order, which is the order for which not only the WCRFS model and the MC lead to similar number of instabilities but covers the frequency of the dominant mode.

Table II also shows that the unstable trajectories increase significantly between 0.375 and 0.475 Hz. Remarkably, this range of frequencies does not include the frequency of the dominant mode in Table III. It is relevant to note that in all realizations for which the system collapses, the instability is due to an increase of the load consumption that leads to the saturation of the AVRs of the power plants. The modification of the eigenvalue corresponding to the critical electro-mechanical modes (i.e., modes 1 to 3 in Table III) for various saturations of the AVRs are calculated and analyzed. Results indicate that, for different AVRs saturation scenarios, the frequency of the least damped modes does not change significantly and they are all stable. The instability, thus, is not related to the critical electro-mechanical modes, but rather to mode 4, which is linked to the dynamics of the AVRs of all machines but mostly to those of machines 3 and 4 in area 2. We also note that when the AVRs of machine 3 and 4 of those of machines 1 and 2 saturate, then the system become unstable (one real positive eigenvalue in steady-state) which drives the system to voltage collapse.

The modular structure of the WCRFS model allows determining the specific window of harmonics of the noise that causes the instability. We proceed as follows. First we set the order of WCRFS

TABLE III
LEAST DAMPED MODES AND CORRESPONDING FREQUENCY, DAMPING AND MOST PARTICIPATING AREA

Mode	Eigenvalue	f [Hz]	Damping [%]	Area
1	$-0.322 \pm j7.224$	1.150	4.45	2
2	$-0.320 \pm j7.077$	1.126	4.52	1
3	$-0.204 \pm j3.051$	0.486	6.65	2
4	$-0.691 \pm j1.526$	0.243	41.26	2

TABLE IV
NUMBER OF UNSTABLE TRAJECTORIES AFTER REMOVING WCRFS FREQUENCY WINDOWS

Removed harmonics	Removed freq. window [Hz]	# of unstable trajectories
140-150	0.350-0.375	156
150-160	0.375-0.400	120
160-170	0.400-0.425	89
170-180	0.425-0.450	180
180-190	0.450-0.475	230
190-200	0.475-0.500	233

to 500 to reproduce precisely the dynamic effects of the original OUP process on the system. Then, we systematically remove a window of frequencies from the WCRFS model. The removed window does not modify the overall statistical properties of the process, nevertheless can significantly change the effect of such a noise on the system dynamic response.

Table IV shows that the most critical range of frequencies that affects the stability of the system is between 0.4 and 0.425 Hz. This range is roughly a multiple of the frequency of mode 4 when an AVR saturates (see Table V). As the nonlinearity of the system is retained, the frequency relationship is not exactly the same or multiple. The sequence of event is thus as follows: for some realizations, the load power consumption increases above a certain threshold; this triggers the saturation of one of the AVRs of the power plants. Depending on the frequencies included in the WCRFS model, the dynamics of the remaining AVRs can be less damped until, eventually an additional AVR saturates thus leading the system to the collapse. On the other hand, removing the range of frequencies between 0.475 and 0.5 Hz, that is, the frequencies around that critical inter-area modes of the system, does not significantly impact the number of unstable simulations which means the generalized forced oscillation [4] is not the main cause of the system instability.

Note that retaining nonlinearity is an advantage of the proposed method with respect to existing techniques which are linear or based on linearized methods, e.g., [4], [5]. Moreover, as the proposed method analyzes the system stability through numerical simulation, it can be utilized for any unstable phenomenon triggered by noise, such as AVR saturation in our second case study or generalized forced oscillation [4]. The generation of the WCRFS of Wiener processes is a relatively inexpensive technique and, if needed, it can be easily parallelized. In this specific study, the number of buses and modes of the system does not impact on the robustness or on the conclusions. The proposed method is applicable to any stochastic process that is constructed starting from a Wiener process, thus including processes with non-Gaussian distributions (e.g. Weibull, Gamma, etc.) and non-exponential autocorrelation.

IV. CONCLUSIONS

The letter proposes the utilization of WCRFS theory to model stochastic processes. This model can be made perfectly equivalent to Wiener processes in terms of statistical properties, provided that a sufficient number of harmonics is considered. We also show however, that not all harmonics are equally relevant. The WCRFS model allows identifying which harmonics are most critical for the system. These are not trivially the ones associated with the least damped mode of the system. Future work will focus on exploiting the diagnostic features of the WCRFS model and designing corrective actions e.g., the implementation of band-stop filters or parameter adjustment, to improve the system stability. Another relevant future work direction is the study of data-based Gaussian and non-Gaussian stochastic processes. Finally, we will also further investigate on the convergence analysis and simulation verification of different expansion forms of the Wiener process.

TABLE V
MODIFICATION OF THE EIGENVALUE CORRESPONDING TO MODE 4 FOR VARIOUS SATURATIONS OF THE AVRS

Eigenvalue	f [Hz]	Damping [%]	AVRs
$-0.691 \pm j1.526$	0.243	41.26	All
$-0.496 \pm j1.241$	0.213	37.13	2, 3, 4
$-0.436 \pm j1.097$	0.188	36.92	1, 3, 4
$-0.503 \pm j1.193$	0.190	38.83	1, 2, 4
$-0.440 \pm j1.033$	0.164	39.19	1, 2, 3

REFERENCES

[1] F. Milano *et al.*, "Power system modelling as stochastic functional hybrid differential-algebraic equations," *IET Smart Grid*, vol. 5, no. 5, pp. 309–331, 2022.

[2] M. Adeen and F. Milano, "On the impact of auto-correlation of stochastic processes on the transient behavior of power systems," *IEEE Trans. on Power Systems*, vol. 36, no. 5, pp. 4832–4835, 2021.

[3] G. Pierrou and X. Wang, "Analytical study of the impacts of stochastic load fluctuation on the dynamic voltage stability margin using bifurcation theory," *IEEE Trans. on Circuits and Systems I: Regular Papers*, vol. 67, no. 4, pp. 1286–1295, 2019.

[4] Y. Yu, P. Ju, Y. Peng, B. Lou, and H. Huang, "Analysis of dynamic voltage fluctuation mechanism in interconnected power grid with stochastic power disturbances," *J. of Modern Power Systems and Clean Energy*, vol. 8, no. 1, pp. 38–45, 2019.

[5] H. Li, P. Ju, C. Gan, S. You, F. Wu, and Y. Liu, "Analytic analysis for dynamic system frequency in power systems under uncertain variability," *IEEE Transactions on Power Systems*, vol. 34, no. 2, pp. 982–993, 2018.

[6] M. Badieirostami, A. Adibi, H.-M. Zhou, and S.-N. Chow, "Model for efficient simulation of spatially incoherent light using the wiener chaos expansion method," *Optics letters*, vol. 32, no. 21, pp. 3188–3190, 2007.

[7] H. C. Ozen and G. Bal, "Dynamical polynomial chaos expansions and long time evolution of differential equations with random forcing," *SIAM/ASA Journal on Uncertainty Quantification*, vol. 4, no. 1, pp. 609–635, 2016.

[8] Y. Qiu, J. Lin, X. Chen, F. Liu, and Y. Song, "Nonintrusive uncertainty quantification of dynamic power systems subject to stochastic excitations," *IEEE Trans. on Power Systems*, vol. 36, no. 1, pp. 402–414, 2021.

[9] G. M. Jónsdóttir and F. Milano, "Data-based continuous wind speed models with arbitrary probability distribution and autocorrelation," *Renewable Energy*, vol. 143, pp. 368 – 376, 2019.

[10] M. Olsson, M. Perninge, and L. Söder, "Modeling real-time balancing power demands in wind power systems using stochastic differential equations," *Electric Power System Research*, vol. 80, no. 8, pp. 966–974, Aug. 2010.

[11] T. Y. Hou, W. Luo, B. Rozovskii, and H.-M. Zhou, "Wiener chaos expansions and numerical solutions of randomly forced equations of fluid mechanics," *Journal of Computational Physics*, vol. 216, no. 2, pp. 687–706, 2006.

[12] T. Melink and J. Korelc, "Stability of karhunen–loève expansion for the simulation of gaussian stochastic fields using galerkin scheme," *Probabilistic Engineering Mechanics*, vol. 37, pp. 7–15, 2014.

[13] L. C. Evans, *An introduction to stochastic differential equations*. American Mathematical Soc., 2012, vol. 82.

[14] F. Milano, "A Python-based software tool for power system analysis," in *IEEE PES General Meeting*, Vancouver, BC, Jul. 2013.

[15] P. W. Sauer and M. A. Pai, *Power system dynamics and stability*. Prentice Hall, 1998.